Inorg. Chem. **2008**, *47*, 10258−10268

Efficient Sensitization of Europium, Ytterbium, and Neodymium Functionalized Tris-Dipicolinate Lanthanide Complexes through Tunable Charge-Transfer Excited States

Anthony D'Aléo,*,† Alexandre Picot,† Andrew Beeby,‡ J. A. Gareth Williams,‡ Boris Le Guennic,† Chantal Andraud,† and Olivier Maury*,†

Université de Lyon, Laboratoire de Chimie, CNRS - Ecole Normale Supérieure de Lyon UMR 5182, 46 allée d'Italie, 69007 Lyon, France, and Department of Chemistry, Durham University, Durham, DH1 3LE, United Kingdom

Received July 10, 2008

A series of push−pull donor-π-conjugated dipicolinic acid ligands and related tris-dipicolinate europium and lutetium complexes have been prepared. The ligands present broad absorption and emission transitions in the visible spectral range unambiguously assigned to charge-transfer transitions (CT) by means of time-dependent density functional theory calculations. The photophysical properties (absorption, emission, luminescence quantum yield, and lifetime) of the corresponding europium complexes were thoroughly investigated. Solvatochromism and temperature effects clearly confirm that Eu(III) sensitization directly occurs from the ligand CT state. In addition, modulation of the energy of the CT donating state by changing the nature of the donor fragment allows the optimal energy of the antennae for europium sensitization to be determined, and this optimal energy was found to be close to the $^5D_1$ accepting state. Finally, this CT sensitization process has been successfully extended to near-infrared emitters (neodymium and ytterbium).

Introduction

In the field of materials science, lanthanides are elements of growing importance due to their optical and magnetic properties arising from the f-orbital filling.[1−4] At the molecular level, the strong paramagnetism of these ions has found important applications in NMR shift reagents, for instance, for 3D protein structure determination,[5] or in contrast agents for in vivo magnetic resonance imaging.[6] On the other hand, the unique luminescence properties (sharp transitions in the visible or in the near-infrared range with large Stokes shifts, long excited-state lifetimes up to milliseconds, and sensitivity to the local environment) find promising applications in biosensors,[7] fluorescence immunoassay,[8] and luminescent probes for time-resolved microscopy and bioimaging.[9−14] Whereas the linear optical properties of lanthanide compounds have been extensively studied, their potential in nonlinear optics (NLO; second-[15−18] or third-order[19−21]) remains an open field of research. In particular, few articles report the sensitization

* Author to whom correspondence should be addressed. E-mail: olivier.maury@ens-lyon.fr.
† Université de Lyon.
‡ Durham University.

(1) Bünzli, J.-C. G.; Piguet, C. *Chem. Rev.* **2002**, *102*, 1897–1928.
(2) Parker, D.; Dickins, R. S.; Puschmann, H.; Crossland, C.; Howard, J. A. K. *Chem. Rev.* **2002**, *102*, 1977–2010.
(3) Benelli, C.; Gatteschi, D. *Chem. Rev.* **2002**, *102*, 2369–2388.
(4) Tsukube, H.; Shinoda, S. *Chem. Rev.* **2002**, *102*, 2389–2403.
(5) Pintacuda, G.; John, M.; Su, X.-C.; Otting, G. *Acc. Chem. Res.* **2007**, *40*, 206–212.
(6) Caravan, P.; Ellison, J. J.; McMurry, T. J.; Lauffer, R. B. *Chem. Rev.* **1999**, *99*, 2293–2352.
(7) Pandya, S.; Yu, J.; Parker, D. *Dalton Trans.* **2006**, 2757–2766.
(8) Hemmilä, I.; Webb, S. *Drug Discovery Today* **1997**, *2*, 373–381.
(9) Mariott, G.; Clegg, R. M.; Arndt-Jovin, D. J.; Jovin, T. M. *Biophys. J.* **1991**, *60*, 1374–1386.
(10) Beeby, A.; Botchway, S. W.; Clarkson, I. M.; Faulkner, S.; Parker, A. W.; Parker, D.; Williams, J. A. G. *J. Photochem. Photobiol. B* **2000**, *57*, 83–89.
(11) Faulkner, S.; Pope, S. J. A.; Burton-Pye, B. P. *Appl. Spec. Rev.* **2004**, *39*, 1–35.
(12) Yu, J.; Parker, D.; Pal, R.; Poole, R. A.; Cann, M. J. *J. Am. Chem. Soc.* **2006**, *128*, 2294–2299.
(13) Charbonnière, L. J.; Hildebrandt, N.; Ziessel, R.; Löhmannsröben, H. G. *J. Am. Chem. Soc.* **2006**, *128*, 12800–12809.
(14) Aarons, R. J.; Notta, J. K.; Meloni, M. M.; Feng, J.; Vidyasagar, R.; Narvainen, J.; Allan, S.; Spencer, N.; Kauppinen, R. A.; Snaith, J. S.; Faulkner, S. *Chem. Commun.* **2006**, 909–911.
(15) Sénéchal, K.; Toupet, L.; Ledoux, I.; Zyss, J.; Le Bozec, H.; Maury, O. *Chem. Commun.* **2004**, 2180–2181.
(16) Tancrez, N.; Feuvrie, C.; Ledoux, I.; Zyss, J.; Toupet, L.; Le Bozec, H.; Maury, O. *J. Am. Chem. Soc.* **2005**, *127*, 13474–13479.

10.1021/ic8012969 CCC: $40.75
Published on Web 10/21/2008

of Ln emission by two-photon absorption,[22−26] a third-order NLO process, despite the tremendous advantages for bioimaging microscopy that should be possible by combining the advantages of lanthanide luminescence with those of two-photon excitation in the near-infrared region.[27−29] The reason for this limited interest to date is almost certainly related to the Ln sensitization process: high NLO activities are achieved with dipolar, quadrupolar, or octupolar compounds featuring highly polarizable charge transfer (CT) transitions located in the visible part of the spectra, and such transitions have hitherto generally been avoided for sensitization purposes.

In this field, sensitization by the so-called antenna effect is frequently used to overcome the low molar absorption coefficient of the Laporte forbidden f−f transitions ($\varepsilon < 1$ L mol^{-1} cm^{-1}). The sensitization process that populates the metal excited state can proceed via a number of distinct mechanisms. The most commonly encountered involves the triplet excited state of a conjugated ligand (i.e., a nondirectional π^* state also called local excited state ^{3}L),[30−35] which is often efficiently populated and possesses an intrinsically long lifetime, allowing efficient transfer to the lanthanide. For the most readily reduced lanthanides, in particular Yb^{3+}, a stepwise double-electron-transfer pathway, of which the first step is electron transfer from the excited chromophore to the metal, provides an alternative.[36,37] Another pathway, developed more recently, involves the triplet metal-to-ligand charge transfer (^{3}MLCT) states of complexes of transition metal ions such as ruthenium,[38−40] osmium,[41] iridium,[42] platinium,[43,44] rhenium,[45−47] or others,[48] with conjugated ligands. These states frequently possess long excited-state lifetimes, and the high spin−orbit coupling constant of these metal ions promotes the efficient intersystem crossing to the triplet state. A related, elegant, yet synthetically challenging, approach is the use of lanthanide-to-lanthanide energy transfer.[49] Finally, sensitization may also be possible via intraligand CT states. Despite the plethora of studies on photoinduced CT phenomena in organic molecules, their use in the sensitization of lanthanides has been demonstrated to work efficiently only very recently.[50−53]

Since we envisaged the design of lanthanide complexes featuring high nonlinear optical activity, in particular, high two-photon cross-sections combined with optimized quantum yield, we decided to focus our attention on this last sensitization process based on charge transfer transitions. To that end, we prepared a series of push−pull donor-π-conjugated dipicolinic acid ligands (Chart 1) in which the low-energy CT transition is tuned by the nature of the donor group (alkyl, alkoxy, alkylthio, and dialkylamino) and by the nature of the conjugated backbone. The present article describes the optimization of the europium sensitization and the extension of this CT strategy to the near-infrared emitters (neodymium and ytterbium). This study opens the way for the optimization of the two-photon absorption cross-sections of the lanthanide complexes described in the part 2 paper that follows.

(17) Sénéchal, K.; Hemeryck, A.; Tancrez, N.; Toupet, L.; Williams, J. A. G.; Ledoux, I.; Zyss, J.; Boucekkine, A.; Guégan, J.-P.; Le Bozec, H.; Maury, O. *J. Am. Chem. Soc.* **2006**, *128*, 12243–12255.
(18) Bogani, L.; Cavigli, L.; Bernot, K.; Sessoli, R.; Guriolo, M.; Gatteschi, D. *J. Mater. Chem.* **2006**, *16*, 2587–2592.
(19) Wong, K.-L.; Kwok, W.-M.; Wong, W.-T.; Phillips, D. L.; Cheah, K. W. *Angew. Chem., Int. Ed.* **2004**, *43*, 4659–4662.
(20) Hou, H.; Wei, Y.; Song, Y.; Fan, Y.; Zhu, Y. *Inorg. Chem.* **2004**, *43*, 1323–1327.
(21) Law, G.-L.; Kwok, W.-M.; Wong, W.-T.; Wong, K.-L.; Tanner, P. A. *J. Phys. Chem. B* **2007**, *111*, 10858–10861.
(22) Piszczek, G.; Maliwal, B. P.; Gryczynski, I.; Dattelbaum, J.; Lakowicz, J. R. *J. Fluoresc.* **2001**, *11*, 101–107.
(23) White, G. F.; Litvinenko, K. L.; Meech, S. R.; Andrews, D. L.; Thomson, A. J. *Photochem. Photobiol. Sci.* **2004**, *3*, 47–55.
(24) Fu, L.-M.; Wen, X.-F.; Ai, X.-C.; Sun, Y.; Wu, Y.-S.; Zhang, J.-P.; Wang, Y. *Angew. Chem., Int. Ed.* **2005**, *44*, 747–750.
(25) Werts, M. H. V.; Nerambourg, N.; Pélégry, D.; Le Grand, Y.; Blanchard-Desce, M. *Photochem. Photobiol. Sci.* **2005**, *4*, 531–538.
(26) Picot, A.; Malvolti, F.; Le Guennic, B.; Baldeck, P. L.; Williams, J. A. G.; Andraud, C.; Maury, O. *Inorg. Chem.* **2007**, *46*, 2659–2665.
(27) D'Aléo, A.; Pompidor, G.; Elena, B.; Vicat, J.; Baldeck, P. L.; Toupet, L.; Kahn, R.; Andraud, C.; Maury, O. *ChemPhysChem* **2007**, *8*, 2125–2132.
(28) Palsson, L. O.; Pal, R.; Murray, B. S.; Parker, D.; Beeby, A. *Dalton Trans.* **2007**, 5726–5730.
(29) Picot, A.; D'Aléo, A.; Baldeck, P. L.; Grishine, A.; Duperray, A.; Andraud, C.; Maury, O. *J. Am. Chem. Soc.* **2008**, *130*, 1532–1533.
(30) Klink, S. I.; Grave, L.; Reinhoudt, D. N.; van Veggel, F. C. J. M.; Werts, M. H. V. J.; Geurts, F. A. J.; Hofstraat, J. W. *J. Phys. Chem. A* **2000**, *104*, 5457–5468.
(31) Beeby, A.; Faulkner, S.; Parker, D.; Williams, J. A. G. *J. Chem. Soc. Perkins Trans 2* **2001**, 1268–1273.
(32) Klink, S. I.; Hebbink, G. A.; Grave, L.; OudeAlink, P. G. B.; van Veggel, F. C. J. M.; Werts, M. H. V. *J. Phys. Chem. A* **2002**, *106*, 3681–3689.
(33) Shavaleev, N. M.; Pope, S. J. A.; Bell, Z. R.; Faulkner, S.; Ward, M. D. *Dalton Trans.* **2003**, 808–814.
(34) Ronson, T. K.; Adams, H.; Harding, L. P.; Pope, S. J. A.; Sykes, D.; Faulkner, S.; Ward, M. D. *Dalton Trans.* **2007**, 1006–1022.
(35) Binnemans, K. In *Handbook on The Physics and Chemistry of Rare Earths*; Amsterdam, 2005; Vol. 35, Chapter 225.
(36) Horrocks, W. D. W.; Bolender, J. P.; Smith, W. D.; Supkowski, R. M. *J. Am. Chem. Soc.* **1997**, *119*, 5972–5973.
(37) Beeby, A.; Faulkner, S.; Williams, J. A. G. *Dalton Trans.* **2002**, 1918–1922.
(38) Herrera, J.-M.; Pope, S. J. A.; Adams, H.; Faulkner, S.; Ward, M. D. *Inorg. Chem.* **2006**, *45*, 3895–3904.
(39) Sénéchal-David, K.; Pope, S. J. A.; Quinn, S.; Faulkner, S.; Gunnlaugsson, T. *Inorg. Chem.* **2006**, *45*, 10040–10042.
(40) Baca, S. G.; Adams, H.; Sykes, D.; Faulkner, S.; Ward, M. D. *Dalton Trans.* **2007**, 2419–2430.
(41) Pope, S. J. A.; Coe, B. J.; Faulkner, S.; Bichenkova, E. V.; Yu, X.; Douglas, K. T. *J. Am. Chem. Soc.* **2004**, *126*, 9490–9491.
(42) Coppo, P.; Duati, M.; Kozhevnikov, V. N.; Hofstraat, J. W.; De Cola, L. *Angew. Chem., Int. Ed.* **2005**, *44*, 1806–1810.
(43) Shavaleev, N. M.; Morrecraft, L. P.; Pope, S. J. A.; Bell, Z. R.; Faulkner, S.; Ward, M. D. *Chem.—Eur. J.* **2003**, *9*, 5283–5291.
(44) Li, X.-L.; Dai, F.-R.; Zhu, Y.-M.; Peng, Q.; Cheng, Z.-N. *Organometallics* **2007**, *26*, 4483–4490.
(45) Pope, S. J. A.; Coe, B. J.; Faulkner, S. *Chem. Comm.* **2004**, 1550–1551.
(46) Shavaleev, N. M.; Accorsi, G.; Virgili, D.; Bell, Z. R.; Lazarides, T.; Calogero, G.; Armaroli, N.; Ward, M. D. *Inorg. Chem.* **2005**, *44*, 61–72.
(47) Kennedy, F.; Shavaleev, N. M.; Koullourou, T.; Bell, Z. R.; Jeffery, J. C.; Faulkner, S.; Ward, M. D. *Dalton Trans.* **2007**, 1492–1499.
(48) Sambrook, M. R.; Curiel, D.; Hayes, E. J.; Beer, P. D.; Pope, S. J. A.; Faulkner, S. *New J. Chem.* **2006**, *30*, 1133–1136.
(49) Faulkner, S.; Pope, S. J. A. *J. Am. Chem. Soc.* **2003**, *125*, 10526–10527.
(50) Werts, M. H. V.; Duin, M. A.; Hofstraat, J. W.; Verhoeven, J. W. *Chem. Commun.* **1999**, 799–800.
(51) Kim, Y. H.; Baek, N. S.; Kim, H. K. *ChemPhysChem* **2006**, *7*, 213–221.
(52) Nie, D.; Chen, Z.; Bian, Z.; Zhou, J.; Liu, Z.; Chen, F. Y. Z.; Huang, C. *New J. Chem.* **2007**, *31*, 1639–1646.
(53) Kadjane, P.; Charbonnière, L.; Camerel, F.; Lainé, P. P.; Ziessel, R. *J. Fluoresc.* **2008**, *18*, 119–129.

Chart 1. Structures of the Ligands and Schematical Representation of the Corresponding Complexes Synthesized and Investigated

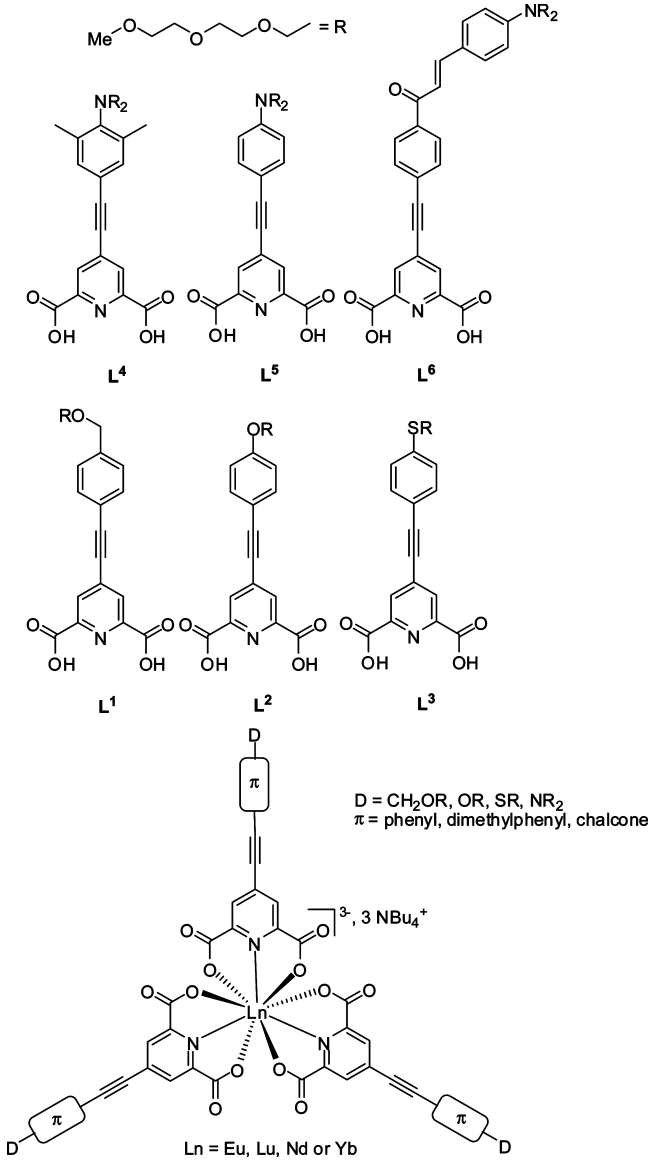

Results and Discussion

1. Synthesis. All of the ligands studied in this article (Chart 1) present the same structure. The dipicolinic acid fragment acts both structurally as a tridentate ligand known to complex 4f ions efficiently[16,27,50,54−56] and electronically as an accepting group. This ligand is functionalized in its 4 position by donor-π-conjugated moieties resulting in the formation of a push−pull molecule (Chart 1). The strength of the donor group can be tuned from alkyl (very weak) to alkoxy (weak) to alkylthio (medium) to dialkylamino (strong), and the length of the conjugated skeleton varies from phenylethynyl ($\mathbf{L^1}$−$\mathbf{L^5}$) to the more extended system of the unusual chalcone-ethynyl derivative ($\mathbf{L^6}$). All of the ligands contain polyethyleneglycol pendants (−R) to ensure solubility both in water and in organic solvents. The properties conferred by such moieties are especially attractive in the practical synthesis of the corresponding $A_3[Ln\mathbf{L}^i_3]$ complexes (Ln = Eu, Lu, Nd, Yb; A represents NBu_4^+). The complexes were prepared in water simply by mixing a solution of the appropriate lanthanide(III) chloride salt with 3 equiv of the ligands, in the presence of NBu_4OH acting as a base and counterion. The complete synthetic procedure and characterization of the ligands and related complexes is described in the part 2 paper and in the Supporting Information.

2. Theoretical Calculations. Density functional theory (DFT) calculations using the B3LYP functional were performed on the ligands $\mathbf{L}^{i\prime}$ (i = 1−6) featuring simplified $-OCH_2CH_2OMe$ end groups. Geometrical optimization of $\mathbf{L^{1\prime}}$−$\mathbf{L^{5\prime}}$ containing the phenylene−ethynylene backbone reveals a completely planar structure similar to that obtained by X-ray crystallography in the case of related dipicolinic amide ligands.[57] Selected frontier molecular orbital diagrams of the ligands $\mathbf{L^{1\prime}}$, $\mathbf{L^{4\prime}}$, $\mathbf{L^{5\prime}}$, and $\mathbf{L^{6\prime}}$ are depicted in Figure 1. Interestingly, in the case of $\mathbf{L^{4\prime}}$, the steric repulsion between the two methyl groups and the dialkylamino fragment forces the molecule to adopt a conformation where the nitrogen electronic lone pair is nearly perpendicular to the conjugated system (twist angle is calculated to be 89°). Thus, contrary to $\mathbf{L^{5\prime}}$, there is no significant conjugation in the ground state between the amino donor group and the pyridinic fragment.[58,59] Ligand $\mathbf{L^{6\prime}}$, featuring an extended ethynyl−chalcone skeleton, presents a structure very close to planarity (twist angle is estimated to be less than 15°), indicating that the conjugation between the electron-donating and -withdrawing groups remains excellent.

3. UV/Vis Absorption Spectroscopy. The UV/vis absorption spectra of ligands were recorded in a dichloromethane solution and are depicted in Figure 2 and Table 1. All chromophores exhibit broad, intense, structureless, low-energy absorption transitions in the visible part of the spectra, with λ_{max} between 323 and 438 nm, depending on the nature of the donor and linker groups. For all ligands, time-dependent density functional theory (TD-DFT) calculations indicate that this lowest-energy transition can be unambiguously assigned to a CT transition, the highest occupied molecular orbital (HOMO) and lowest unoccupied molecular orbital (LUMO) being localized on the donor and acceptor group, respectively (Figure 1). The calculated maximal absorption wavelength, λ_{max}^{calcd}, matches almost perfectly with the experimental one (Table 1). It is worth noting that, in the case of $\mathbf{L^{1\prime}}$, the HOMO is delocalized along the π system due to the very weak electron-donating character of the methylene fragment, and therefore the lowest energy transition has mixed parentage between CT and π−π* transition

(54) Renaud, F.; Piguet, C.; Bernardinelli, G.; Bünzli, J.-C. G.; Hopfgartner, G. *Chem.−Eur. J.* **1997**, *3*, 1646–1659.
(55) Binnemans, K.; Van Herck, K.; Görller-Wallrand, C. *Chem. Phys. Lett.* **1997**, *266*, 297–302.
(56) D'Aléo, A.; Toupet, L.; Rigaut, S.; Andraud, C.; Maury, O. *Opt. Mater.* **2008**, *30*, 1682−1688.
(57) Picot, A.; Feuvrie, C.; Barsu, C.; Le Guennic, B.; Malvolti, F.; Le Bozec, H.; Andraud, C.; Toupet, L.; Maury, O. *Tetrahedron* **2008**, *64*, 399–411.
(58) Grabowski, Z. R.; Rotkiewicz, K.; Rettig, W. *Chem. Rev.* **2003**, *103*, 3899–4031.
(59) Hao, R.; Li, M.; Wang, Y.; Zhang, J.; Ma, Y.; Fu, L.; Wen, X.; Wu, Y.; Ai, X.; Zhang, S.; Wei, Y. *Adv. Funct. Mat.* **2007**, *17*, 3663–3669.

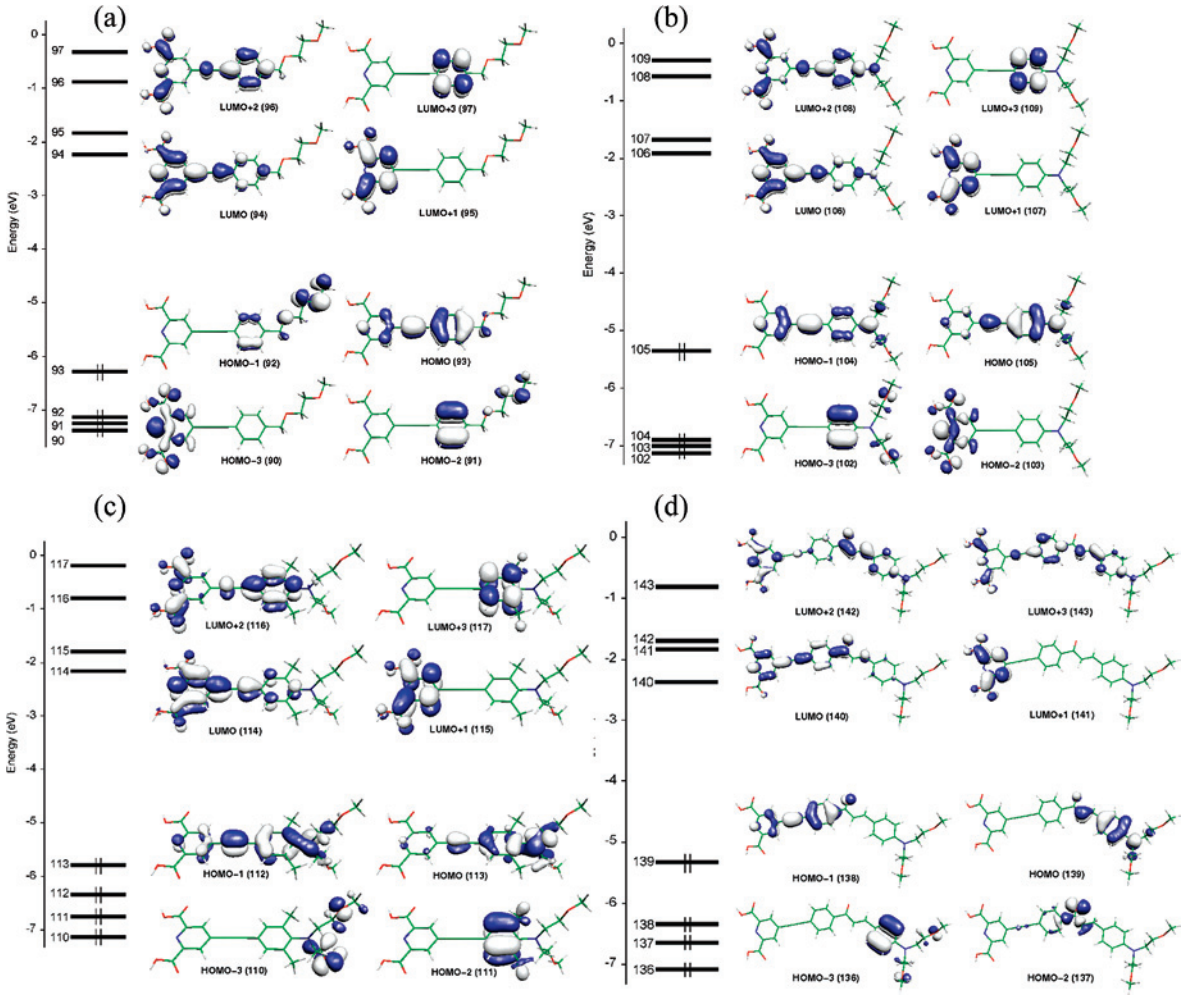

Figure 1. MO diagrams of (a) $\mathbf{L}^{1'}$, (b) $\mathbf{L}^{5'}$, (c) $\mathbf{L}^{4'}$, and (d) $\mathbf{L}^{6'}$.

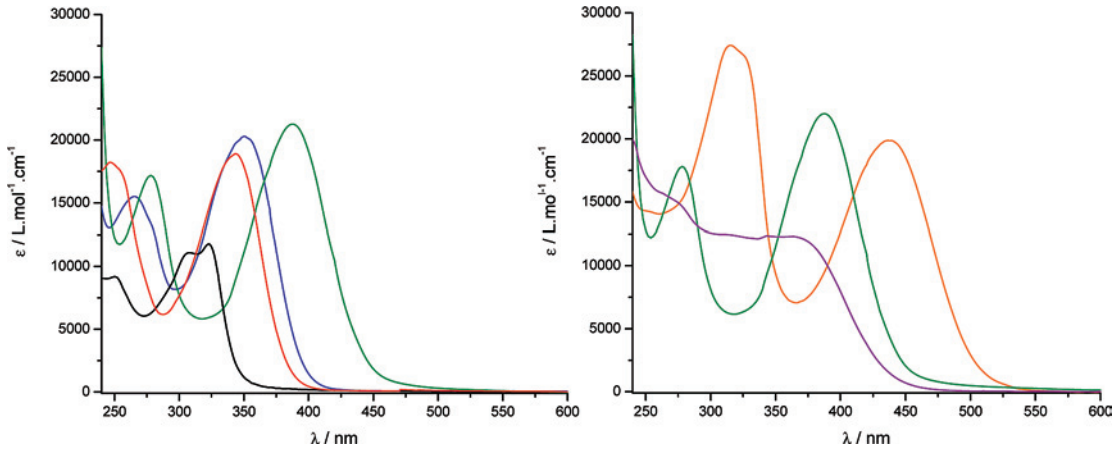

Figure 2. UV/vis absorption spectra in dichloromethane of (left) $\mathbf{L}^{1}$ (black), $\mathbf{L}^{2}$ (red), $\mathbf{L}^{3}$ (blue), and $\mathbf{L}^{5}$ (green) and (right) of $\mathbf{L}^{4}$ (purple), $\mathbf{L}^{5}$ (green), and $\mathbf{L}^{6}$ (orange).

character. As expected, increasing the donor strength (from $\mathbf{L}^{1}$ through to $\mathbf{L}^{5}$) or lengthening the π-conjugated backbone ($\mathbf{L}^{6}$) results in a bathochromic shift of the absorption bands (Figure 2). Interestingly, in the case of $\mathbf{L}^{4}$, the twist of the nitrogen lone pair induced by the two flanking methyls results in a blue shift and a broadening of the absorbing CT transition (Figure 2).[59] This behavior, characteristic of a twisted intramolecular charge transfer transition,[58] is confirmed by the theoretical simulation on $\mathbf{L}^{4'}$ (Figure 1): in spite of the twisted ground-state structure, the lowest-energy transition is comprised of mainly two monoexcitations, HOMO → LUMO and HOMO(-1) → LUMO, which both conserve a marked CT character but with a reduced oscillator strength *f* compared to $\mathbf{L}^{5'}$ (Table 1).

Table 1. UV/Vis Absorption and Fluorescence Data of Ligands $\mathbf{L^1}-\mathbf{L^6}$ in Dichloromethane Solution and Corresponding Data Calculated Using TD-DFT for the Ligands $\mathbf{L^{1'}}-\mathbf{L^{6'}}$ in the Gas Phase

	λ_{max} (nm)	ε^{max} ($M^{-1}\cdot cm^{-1}$)	λ_{em} (nm)	ϕ_L	λ_{max}^{calcd} (nm)	f^b	assignment
$\mathbf{L^1}$	323	12000	385	0.23[c]	327	0.84	HOMO → LUMO
$\mathbf{L^2}$	348	19000	483	0.16[c]	344	0.81	HOMO → LUMO
$\mathbf{L^3}$	354	20300	504	0.27[c]	364	0.82	HOMO → LUMO
$\mathbf{L^4}$	374	12300	570	0.011[c]	377	0.34	HOMO → LUMO
							HOMO(−1) → LUMO
$\mathbf{L^5}$	388	22000	580	0.0028[d]	386	0.82	HOMO → LUMO
$\mathbf{L^6}$	438	19500	597	0.0067[d]	457	0.43	HOMO → LUMO

[a] Wavelength of the lowest-energy absorption band calculated by TD-DFT. [b] Calculated oscillator strength of the pertinent transition. [c] Measured using quinine bisulfate in 1 M sulfuric acid solution as a standard. [d] Measured using $[Ru(bpy)_3]Cl_2$ in water as a standard.

Table 2. UV/Vis Absorption and Luminescence Data of $A_3(Ln\mathbf{L}^i_3)$ Complexes ($i = 1-6$ and Ln = Lu, Eu) in Dichloromethane Solution at Room Temperature

	λ_{abs}^{max} (nm)	ε^{max} ($L\cdot mol^{-1}\cdot cm^{-1}$)	λ_{em}^{max} (nm)	ϕ_{CT}^{Ln}[a]	ϕ_{Eu}	τ_{Eu} (ms)	fwhm (cm^{-1})
$A_3(Lu\mathbf{L^1}_3)$	304	64200	386	0.11[b]	[c]	[c]	5100
$A_3(Lu\mathbf{L^2}_3)$	321	84000	435	0.19[b]	[c]	[c]	6200
$A_3(Lu\mathbf{L^3}_3)$	331	76500	504	0.53[b]	[c]	[c]	6400
$A_3(Lu\mathbf{L^4}_3)$	340	47800	466	0.49[b]	[c]	[c]	6500
$A_3(Lu\mathbf{L^5}_3)$	372	94100	545	0.042[d]	[c]	[c]	4800
$A_3(Lu\mathbf{L^6}_3)$	433	89100	583	0.014[d]	[c]	[c]	3300
$A_3(Eu\mathbf{L^1}_3)$	312	61300	613	0.0075[b]	0.059[d]	0.86	
$A_3(Eu\mathbf{L^2}_3)$	321	92000	613	0.0076[b]	0.15[d]	1.90	
$A_3(Eu\mathbf{L^3}_3)$	322	79000	613	0.038[b]	0.43[d]	1.42	
$A_3(Eu\mathbf{L^4}_3)$	318	58500	613	0.016[b]	0.27[d]	1.81	
$A_3(Eu\mathbf{L^5}_3)$	370	89200	613	0.010[d]	0.070[d]	0.85	
$A_3(Eu\mathbf{L^6}_3)$	427	94000	565	0.070[d]	[e]	[e]	

[a] ϕ_{CT}^{Lu} represents the total quantum yield of emission for the Lu complexes, and ϕ_{CT}^{Eu} represents the quantum yield of the residual ligand-centered fluorescence emission from the CT excited state for the Eu complexes, for which ϕ_{Eu} is the quantum yield of metal-based luminescence. [b] Measured using quinine bisulfate in a 1 M sulfuric acid solution as standard. [c] No emission from the lanthanide is possible. [d] Measured using $[Ru(bpy)_3]Cl_2$ in water as a standard. [e] No emission from the Eu is observed at RT.

For all of the ligands, complexation to lutetium(III) ($4f^{14}$, chosen as a control Ln^{3+} ion with no f−f excited states) results in a small blue shift of the maxima of absorption with respect to that of the ligand (Table 2). This effect can be attributed to the trianionic charge of the complexes: the +3 charge of the Lewis acidic lanthanide ion being compensated by the formal −2 charge on each ligand. Replacing Lu with Eu, Nd, or Yb has only a very small influence on the absorption maximum wavelength, indicating that the nature of the metal plays only a very minor role on the ground-state properties of the complexes. The relative effects induced by the ligand modifications are the same in the case of the complexes as those for the ligands (Figure 3a,b), and no significant effect of the solvent polarity is observed on the spectra of the complexes.

4. Luminescence Properties of the Ligands and Lutetium Complexes. The corrected fluorescence emission spectra of the ligands and the corresponding Lu complexes were found to be independent of the excitation wavelength, for all solvents studied. No influence of dissolved molecular oxygen was found, confirming the singlet character of the described transition with a short natural lifetime. The emission bands are broad and structureless, and the large Stokes shifts observed at room temperature confirm the CT assignment of the transition.[60] As expected for emitting CT states, the maximum emission wavelength red-shifts when the donor strength increases, both for the ligands (Table 1) and for the Lu complexes (Table 2 and Figure 4). The fluorescence quantum yields of the Lu complexes decrease from 0.54 to 0.014, the lowest values being observed for those compounds which have the lowest-lying CT excited states (Tables 1 and 2).

Since Lu^{III}, featuring an f^{14} electronic configuration, is spectroscopically inert, the lutetium complexes were used as the reference to determine the energy level of the relaxed CT state emission. The emission maximum energy values (quoted to the nearest 100 cm^{-1}), called E_{CT}, will be used as an approximation for the energy of the relaxed CT state in the Eu analogs. Although gadolinium complexes are often used for this purpose because of the similarity in ionic radii of Eu^{3+} and Gd^{3+}, the lutetium complexes were preferred here to facilitate full characterization by ^1H and ^{13}C NMR spectra (Supporting Information). The errors due to this approximation can be estimated by comparison of the emission of the Lu^{3+} and Eu^{3+} complexes of $\mathbf{L^6}$ (which is unable to sensitize the Eu^{3+} excited state): $\lambda_{em}^{max} = 583$ and 565 nm, respectively. This difference is certainly due to the smaller ionic radius and hence more Lewis acidic nature of the Lu^{3+} ion.

5. Luminescence Properties of Europium Complexes. The characteristic Eu^{III} emission is observed for $A_3(Eu\mathbf{L}^i_3)$ ($i = 1-5$) complexes upon excitation in the CT transition. In the particular case of $A_3(Eu\mathbf{L^6}_3)$, only the broad unstructured emission at 565 nm—similar in shape to that of the Lu analog—is observed, indicating that, for the chalcone derivative, the emission arises only from the CT state and no europium sensitization occurs at room temperature. The quantum yield of Eu luminescence varies from 0.059 for $A_3(Eu\mathbf{L^1}_3)$ to 0.43 for $A_3(Eu\mathbf{L^3}_3)$. For $A_3[Eu\mathbf{L}^i_3]$ ($i = 1-5$), it is interesting to note that the luminescence quantum yields vary in the same way as the fluorescence quantum yields of the Lu complexes. This suggests that these two parameters are somehow related.

To get a better insight into the mechanism of the sensitization, a solvatochromic study of $A_3(Lu\mathbf{L^5}_3)$ and $A_3(Eu\mathbf{L^5}_3)$ was performed in various chlorinated solvents of increasing polarity, for example, chloroform ($\Delta f = 0.251$), 1,1,1-trichloroethane (TCE; $\Delta f = 0.300$), dichloromethane (DCM; $\Delta f = 0.319$) and 1,2-dichloroethane (DCE; $\Delta f = 0.326$), where Δf is the polarity function which is determined by the static and optical dielectric constants ε and n.[2,61,62] As can be seen from Figure 5, upon increasing the polarity of the solvent, the CT maximum emission of the lutetium

(60) At low temperatures, the initially fluidic solution becomes a glassy solid matrix, and the increased medium viscosity associated with the lack of molecular motion in such a medium also contributes to the increase of the CT energy level, avoiding reorganization of the solvent around the excited molecule. Lakowicz, J. R. *Principle of Fluorescence Spectroscopy*; 2nd ed.; Kluwer Academic/Plenum Publishers: New York, 1999.

(61) The solvatochromic study was restricted to chlorinated solvents because the use of other organic solvents such as THF and acetonitrile gives surprising results that can be attributed to the unknown behavior of the polyethylenglycol moieties is such solvents.

(62) Onsager, L. *J. Am. Chem. Soc.* **1936**, *58*, 1486–1493.

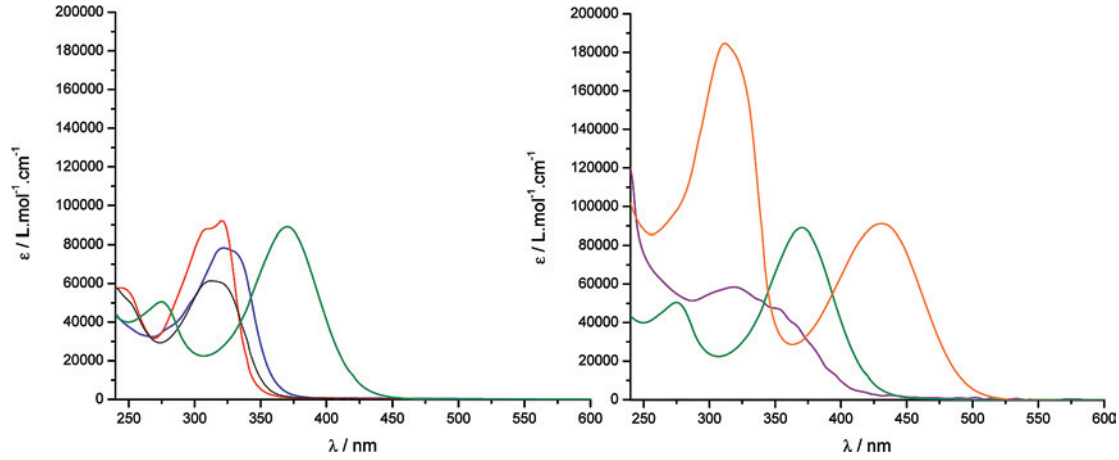

Figure 3. UV/vis absorption spectra in a dichloromethane solution of (left) $A_3(Eu\mathbf{L}^1{}_3)$ (black), $A_3(Eu\mathbf{L}^2{}_3)$ (red), $A_3(Eu\mathbf{L}^3{}_3)$ (blue), and $A_3(Eu\mathbf{L}^5{}_3)$ (green) and (right) of $A_3(Eu\mathbf{L}^4{}_3)$ (purple), $A_3(Eu\mathbf{L}^5{}_3)$ (green), and $A_3(Eu\mathbf{L}^6{}_3)$ (orange).

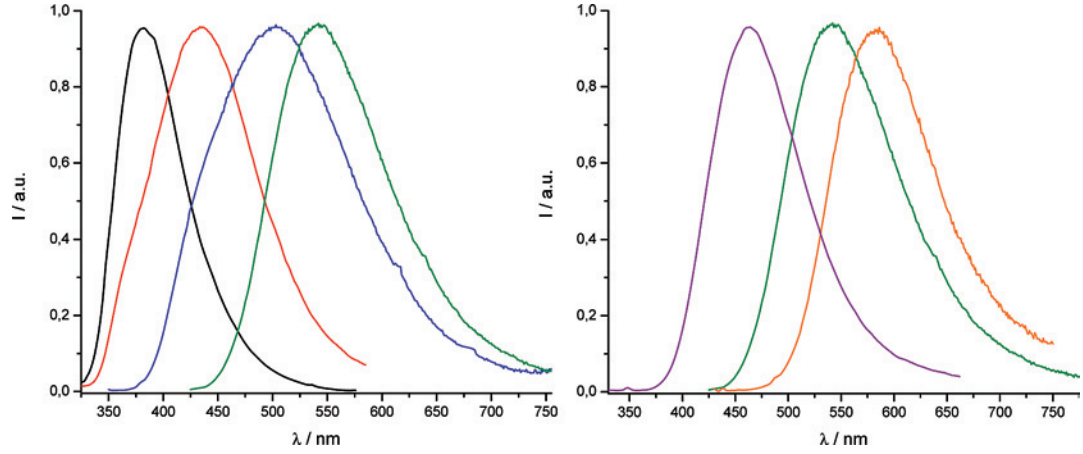

Figure 4. Luminescence spectra in a dichloromethane solution of (left) $A_3(Lu\mathbf{L}^1{}_3)$ (black), $A_3(Lu\mathbf{L}^2{}_3)$ (red; $\lambda_{ex} = 310$ nm), $A_3(Lu\mathbf{L}^3{}_3)$ (blue; $\lambda_{ex} = 340$ nm), and $A_3(Lu\mathbf{L}^5{}_3)$ (green; $\lambda_{ex} = 400$ nm) and of (right) $A_3(Lu\mathbf{L}^4{}_3)$ (purple; $\lambda_{ex} = 330$ nm), $A_3(Lu\mathbf{L}^5{}_3)$ (green), and $A_3(Lu\mathbf{L}^6{}_3)$ (orange; $\lambda_{ex} = 400$ nm).

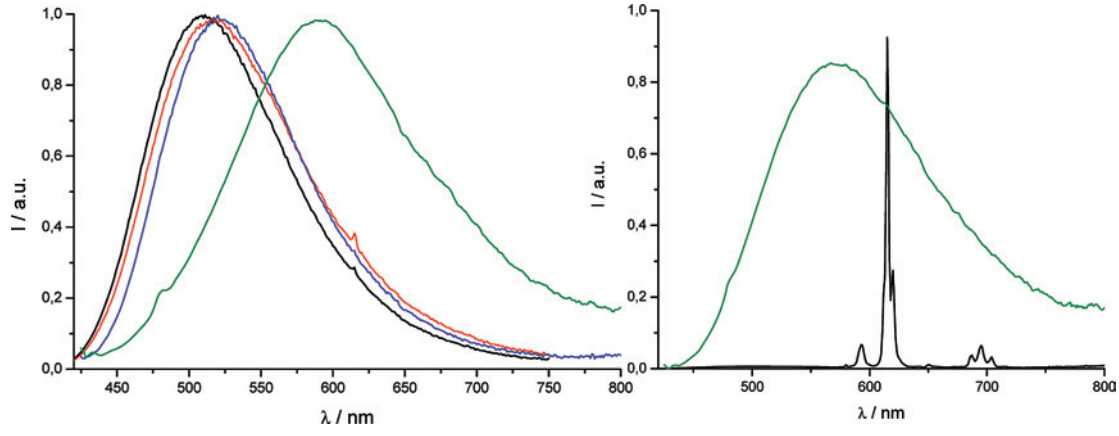

Figure 5. Room temperature emission of $A_3(Lu\mathbf{L}^5{}_3)$ in chloroform (black), TCE (red), DCM (blue), and DCE (green) ($\lambda_{ex} = 360$nm) (left). Room temperature emission of $A_3(Eu\mathbf{L}^5{}_3)$ in chloroform, TCE, DCM (black) and DCE (green) ($\lambda_{ex} = 360$ nm) (right).

complex is increasingly red-shifted from 511 nm in chloroform to 591 nm in DCE. Interestingly, for $A_3(Eu\mathbf{L}^5{}_3)$, the characteristic emission profile of the europium is obtained in all cases except in DCE solution, where only the broad CT emission is observed (Figure 5). Since localized triplet state emissions are less sensitive to solvent polarity effects, these results are in agreement with a sensitization process occurring through the CT state. Similar sensitization of Eu^{III} by a charge-transfer process has recently been evidenced by Kim and co-workers in Eu(terpy)$(NA)_3$ {NA = 4-[4-(4-methoxyphenyl)-naphthalen-1-yl]-benzoic acid}.[51] In the present example, the energy level of the relaxed CT state decreases as the solvent polarity increases and, at a certain energy (in the case of DCE where $E_{CT} = 17\,500$ cm^{-1},

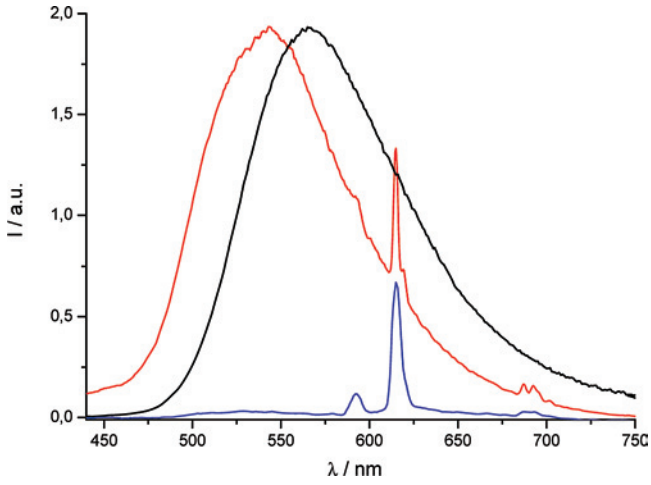

Figure 6. Steady-state emission spectrum of $A_3(Eu\mathbf{L}^6_3)$ at room temperature (black), at 77 K in ethanol/methanol (4/1) glass (red), and time-resolved emission spectrum under the latter conditions (blue) with a delay of 50 μs (λ_{ex} = 400 nm).

λ_{em}^{max} = 570 nm), becomes too low to sensitize the Eu^{III} excited states or, if it does so, is immediately followed by back energy transfer to the ligand.

Furthermore, CT transitions are often known to be thermally activated processes, and as a consequence, lowering the temperature results in an increase of the CT energy level.[60] This effect can be easily verified in the case of $A_3[Eu\mathbf{L}^6_3]$: at room temperature, only the CT emission is observed, as noted earlier (E_{CT} = 17 700 cm^{-1}, λ_{em}^{max} = 565 nm); on the contrary, cooling the sample to 77 K in a solid matrix results in a 20 nm blue-shift of the residual CT emission (E_{CT} = 18 400 cm^{-1}, λ_{em}^{max} = 543 nm), and the emergence of superimposed narrow bands due to the Eu^{III} emission (Figure 6, red line). The latter can be probed more readily by applying a delay of 50 μs in the acquisition of the spectrum, which gates out the short-lived CT emission (Figure 6, blue line). This experiment shows that it is possible to tune the CT energy level not only according to the solvent, but also with the temperature; europium sensitization is impossible at room temperature but recovered at low temperatures.

At this stage, it is possible to propose that, in the $A_3(Eu\mathbf{L}^i_3)$ family (i = 1−6), the sensitization of europium luminescence occurs from the relaxed CT state (Scheme 1). Note that such a CT sensitization process implicitly suggests that the energy of the CT state is even lower than the ligand triplet state. Unfortunately, precise localization of the triplet state by low-temperature emission measurements on lutetium complexes fails due to overlap with the residual CT band. Therefore, in the present case, the CT sensitization hypothesis seems reasonable, although sensitization via triplet state cannot be rigorously ruled out. In addition, solvatochromism and variable-temperature experiments show that it is possible to tune the CT energy level and indicate the existence of a limit below which sensitization no longer occurs. When all of the experimental data are combined, this CT sensitization limit can be estimated between 18 400 and 17 500 cm^{-1}, corresponding to the lowest energy for which Eu^{III} emission occurs ($A_3(Eu\mathbf{L}^6_3)$ at 77 K) and the highest one for which no more

Scheme 1. Schematic Representation of the Process Studied, Where k_1 is the Rate Constant of Nonradiative Decay of the CT State and k_{tr} and k_{btr} Are the Rate Constants of Energy Transfer and Back Transfer, Respectively

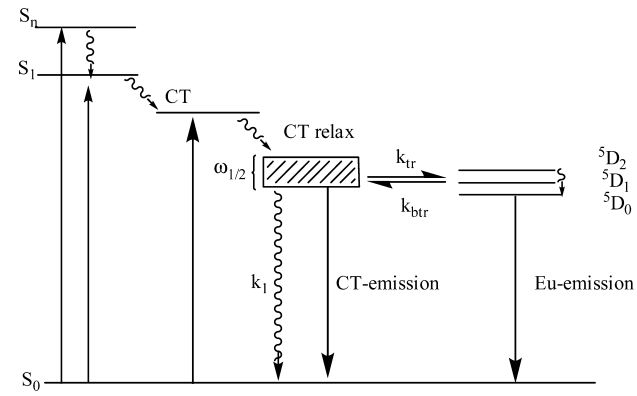

sensitization is possible ($A_3(Eu\mathbf{L}^5_3)$ in DCE), respectively. Not surprisingly, this limit is found just above the Eu^{III} $^5D_0$ emitting level (E = 17 400 cm^{-1}).

6. Quantitative Determination of the Optimized Eu^{III} Sensitization Conditions. After the determination of the lower limit for the sensitization of europium luminescence, we believe that it is important to determine the optimized sensitization conditions. To that end, a study using the Eu and Lu complexes of $\mathbf{L}^1$−$\mathbf{L}^5$, where the nature of the donor group changes the energy of the CT state, was undertaken. In these complexes, the antenna presents the same π-conjugated backbone (same distance between the donor and the acceptor moieties), the only variable being the nature of the donor group. As before, the energy level of the relaxed CT state is estimated using the Lu complexes at room temperature. Since the broad character of the Lu CT emission bands cannot be described using the maximum energy of the transition alone, we have chosen to model this parameter using the full-width half-maximum value (fwhm or $\omega_{1/2}$) to better represent the "thickness" of the relaxed CT emissive state (Scheme 1). Figure 7 represents the dependence of the Eu luminescence lifetime and quantum yield as a function of the position of the CT state.

The lifetimes vary from a few hundred microseconds to 2 μs (Table 2). This variation as a function of the CT energy reveals an increase of the lifetime followed by a decrease. The maximum is obtained for $A_3[Eu\mathbf{L}^2_3]$ in DCM (E_{CT} = 23 000 ± 3100 cm^{-1} for the lutetium analogues). This energy range contains the europium $^5D_2$ excited state, and therefore $^5D_1$ can be considered as the first available accepting state. This result suggests that, when the CT transition is around the energy of the latter state, the Eu lifetime is optimum and the transfer is the most efficient (Figure 7). For $A_3[Eu\mathbf{L}^3_3]$ and $A_3[Eu\mathbf{L}^4_3]$, the luminescence lifetimes are still rather high while the CT energy range contains the $^5D_1$ state. It is important to note that a significant decrease of lifetime is observed when the CT energy range approaches or contains the emissive $^5D_0$ state, as in the case of $A_3[Eu\mathbf{L}^5_3]$. This result is certainly due to the occurrence of back-energy transfer from the Eu $^5D_0$ state to the CT state. The europium luminescence quantum yield follows the same kind of variation with the CT state energy level as the lifetime

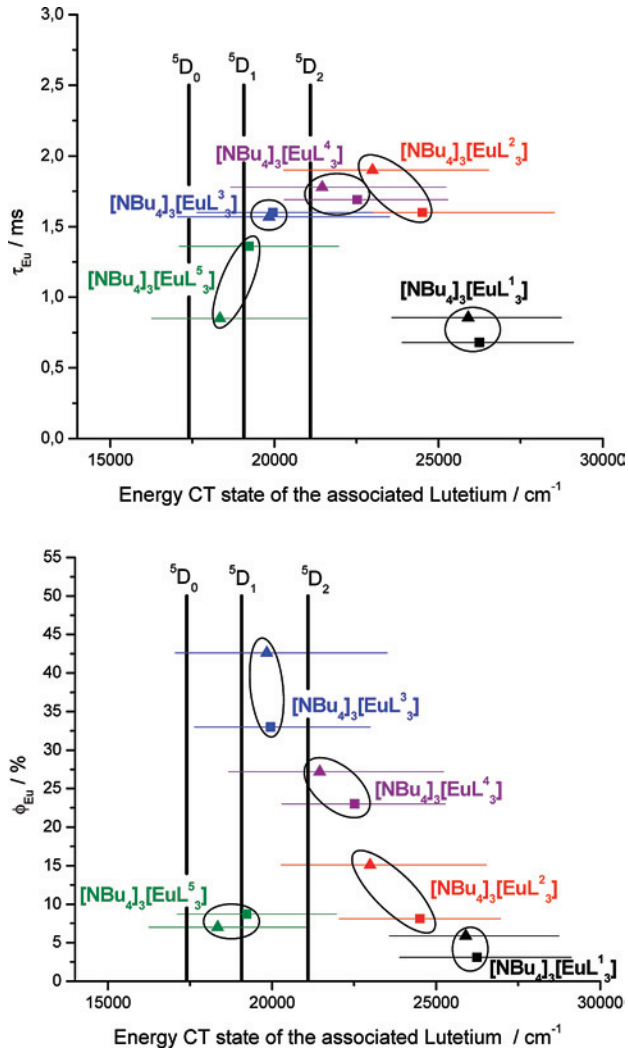

Figure 7. Variation of the Eu luminescence lifetimes (τ_{Eu}, upper) and quantum yields (ϕ_{Eu}, lower) for $A_3[Eu\mathbf{L}^i{}_3]$, ($i = 1-5$) as a function of the position of the CT state of the corresponding lutetium complex. □ and ▲ represent chloroform and DCM solutions, respectively (the straight line representing the full-width at half-maximum).

(Figure 7): a regular increase in Φ_{Eu} with decreasing E_{CT} up to a maximum, followed by a rapid decrease when E_{CT} approaches the $^5D_0$ state. For the quantum yield variation, the maximum is obtained for $A_3[Eu\mathbf{L}^3{}_3]$ in DCM ($\phi_{Eu} = 0.43$, with an E_{CT} value of 19 800 ± 3200 cm^{-1}), a significantly lower sensitizer energy than that obtained for the lifetime maximum (E_{CT} = 23 000 ± 3100 cm^{-1}). Keeping in mind that the luminescence quantum yields of the Eu and Lu complexes vary similarly (vide supra), it seems that both the chemical nature of the antenna and the position of the antenna CT state play an important role in determining the overall Eu quantum yield. These two correlations confirm that europium sensitization occurs through the low-lying CT excited state and unambiguously prove the existence of an optimum antenna energy level for this sensitization. However, the optimal sensitization seems to occur at different energy levels considering either the luminescence lifetimes or the luminescence quantum yields. In order to explain these apparent discrepancies, a thorough study of the kinetic parameters was performed.

The efficiency of the energy transfer (recombination on the Eu transitions) can be estimated by

$$\eta_{ET} = 1 - (\phi_{CT}^{Eu}/\phi_{antenna}^{th}) \quad (1)$$

where ϕ_{CT}^{Eu} is the quantum yield of the residual charge transfer emission in the Eu complexes and $\phi_{antenna}^{th}$ is the theoretical intrinsic quantum yield of the antenna ligand in the europium complex in the absence of any transfer to the metal. The ϕ_{CT}^{Eu} values can be measured from the experimental luminescence spectra (Table 2). Furthermore, following the works of Beeby et al.[63] and of Verhoeven et al.,[50] the efficiency of the sensitization can be estimated using a method defining the overall quantum yield of luminescence (ϕ_{Eu}) as the product of the luminescence quantum yield of the transferring state (the CT state in our case, $\phi_{antenna}^{th}$), the efficiency of the energy transfer (η_{ET}), and the quantum efficiency of metal-centered luminescence (η_{Eu}):

$$\phi_{Eu} = \phi_{antenna}^{th}\eta_{ET}\eta_{Eu} \quad (2)$$

In this equation, $\phi_{antenna}^{th}$ has to be calculated, ϕ_{Eu} is measured, η_{ET} is determined using the above-mentioned procedure (eq 1), and η_{Eu} is calculated using

$$\eta_{Eu} = \tau_{Eu}/\tau_R \quad (3)$$

where τ_{Eu} is the measured Eu lifetime and τ_R is the pure radiative lifetime that can be estimated from the emission spectra as follows:[50,63]

$$k_R = 1/\tau_R = A(0,1)[I_{tot}/I(0,1)] \quad (4)$$

The constant $A(0,1)$ is the spontaneous emission probability of the $^5D_0 \rightarrow {}^7F_1$ transition, equal to 39.4 s^{-1} in DCM, and $I_{tot}/I(0,1)$ is the ratio of the total integrated emission intensity to the intensity of the $^5D_0 \rightarrow {}^7F_1$ transition.

$$\begin{cases} \eta_{ET} = 1 - (\phi_{CT}^{Eu}/\phi_{antenna}^{th}) & (1) \\ \phi_{Eu} = \phi_{antenna}^{th}\eta_{ET}\eta_{Eu} & (2) \end{cases}$$

Equations 1 and 2 form a system of two equations containing two unknown values, $\phi_{antenna}^{th}$ and η_{ET}, that can be easily solved (details of the calculation are given in the Supporting Information). Finally, $\phi_{antenna}^{th}$ and η_{ET} can be expressed as a function of ϕ_{Eu}, η_{Eu}, and ϕ_{CT}^{Eu}, which are parameters determined from experimental data (Table 3).

$$\begin{cases} \phi_{antenna}^{th} = \phi_{Eu}/\eta_{Eu} + \phi_{CT}^{Eu} & (5) \\ \eta_{Eu} = \phi_{antenna}^{th} \cdot \eta_{Eu}/\phi_{Eu} & (6) \end{cases}$$

It is important to note that both values are determined directly from the europium complex emission spectra without any participation of an external model (e.g., a corresponding La, Gd, or Lu complex) as frequently encountered in the literature. The values of η_{ET} are roughly constant and higher than 95% in all of these cases, indicating that the energy transfer is very efficient. Furthermore, the theoretical quantum yield of the antenna in the absence of any transfer, $\phi_{antenna}^{th}$, varies in the same way but remains lower than that

(63) Beeby, A.; Bushby, L. M.; Maffeo, D.; Williams, J. A. G. *J. Chem. Soc., Dalton Trans.* **2002**, 48–54.

Table 3. Calculated Values in Dichloromethane of τ_R, Σk_R, η_{Eu}, and $\phi^{th}_{antenna}$ for $A_3[EuL^i_3]$ ($i = 1-5$) Using Experimentally Determined Quantities τ_{obs}, ϕ_{Eu} and $[I(0,1)/I_{tot}]$

	$A_3[EuL^1_3]$	$A_3[EuL^2_3]$	$A_3[EuL^3_3]$	$A_3[EuL^4_3]$	$A_3[EuL^5_3]$
$[I(0,1)/I_{tot}]$	0.105	0.092	0.087	0.090	0.074
k_R (s^{-1})	375	429	453	438	533
τ_R (ms)	2.66	2.33	2.21	2.28	1.88
τ_{Eu} (ms)	0.86	1.90	1.42	1.81	0.85
η_{Eu}	0.32	0.82	0.64	0.79	0.45
ϕ_{Eu}	0.059	0.15	0.43	0.27	0.070
η_{ET}	0.961	0.960	0.945	0.957	0.937
$\phi^{th}_{antenna}$ [a]	0.19	0.19	0.70	0.36	0.17
Σk_{nr} (s^{-1})	788	97	251	114	643
$\phi^{th}_{antenna}$	0.31	0.79	0.61	0.76	0.42

[a] Estimated uncertainty in $\phi_{Eu} \pm 10\%$, which leads to an uncertainty of this order in $\phi^{th}_{antenna}$.

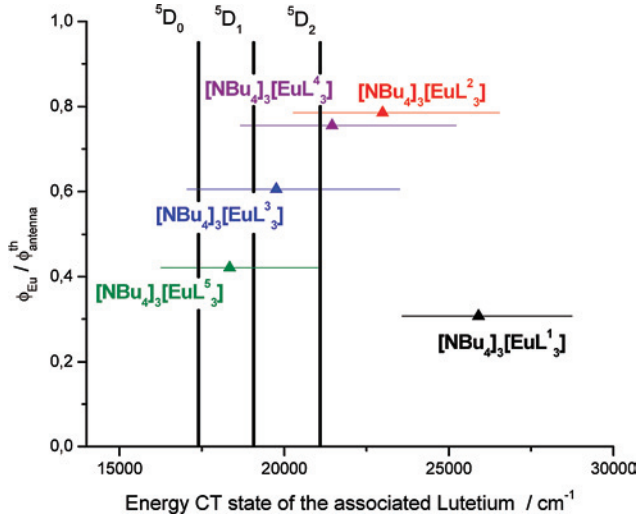

Figure 8. Variation of the Eu luminescence quantum yields normalized by the theoretical antenna quantum yield ($\phi^{th}_{antenna}$) (▲) in dichloromethane for $A_3[EuL^i_3]$ ($i = 1-5$), as a function of the position of the CT state of the associated lutetium complex (the straight line representing the full width at half-maximum).

of the lutetium complexes (ϕ^{Lu}_{CT}, Table 2). Such differences could be explained by the larger size of the europium ion, favoring nonradiative deactivation, and vindicate the present method as a more reliable approach.

Finally, in order to remove the contribution of the chemical structure and to determine the optimal energy of the CT state to populate efficiently the Eu, a representation of $\phi_{Eu}/\phi^{th}_{antenna} = f(E_{CT})$ can be made (Figure 8). In this case, it can be seen that the maximum is reached for $A_3[EuL^2_3]$ ($E_{CT} = 23\,000 \pm 3100$ cm^{-1}), and the variation is very similar to that of the europium emission lifetime τ_{Eu} (Figure 7).

In conclusion of this section, the existence of an optimized CT energy level for Eu^{III} sensitization has been clearly demonstrated. The apparent discrepancies between quantum yield and lifetime can be explained as follows: the Eu^{III} luminescence quantum yield is a global parameter that depends on the energy transfer efficiency *and* on the intrinsic antenna quantum yield (eq 2). On the other hand, the europium luminescence lifetime describes all processes the metal excited state undergoes once populated and, therefore, is correlated to the energy transfer (and back-transfer) efficiency but is not influenced by the intrinsic antenna quantum yield.

Table 4. Photophysical Data of $A_3[LnL^5_3]$ Ln = Lu, Nd, and Yb in Dichloromethane Solution at Room Temperature

	λ^{max}_{abs} (nm)	ε^{max}	λ^{max}_{em} (nm)	$\phi_{CT}{}^{Ln}$	$\tau_{Ln}/\mu s$
$A_3[LuL^5_3]$	372	94100	545	0.118	
$A_3[NdL^5_3]$	368	96100	1064	0.0022	1.2
$A_3[YbL^5_3]$	369	97600	980	0.0059	37

In the present study, the maximum energy transfer efficiency is found for an antenna energy level around 23 000 $\pm$ 3100 cm^{-1}, suggesting that the best accepting level is the $^5D_1$ europium excited state ($^5D_0$ is also a good accepting level, but its longer lifetime as compared to the one of $^5D_1$ allows more time for back energy transfer) and that the best gap between the transferring state and the accepting state is between 2000 and 3000 cm^{-1}. This value seems to be independent of the sensitization process and could be more general (sensitization from ^{3}L, ^{3}MLCT, and Ln states).

7. Luminescence Properties of Ytterbium and Neodymium Complexes. By analogy with the above-described study on Eu complexes, the use of the low-energy CT state of L^5 for the sensitization of Yb and Nd was also envisaged. As a consequence, $A_3[YbL^5_3]$ and $A_3[NdL^5_3]$ were prepared and studied. These complexes exhibit absorption spectra similar to that of the europium or lutetium analog (Figure 3 and Table 4) with a broad, structureless CT transition around 370 nm. Excitation into the CT transition (in DCM solution) induces an emission in the near-infrared (NIR) region which is attributed to the $^2F_{5/2} \rightarrow {}^2F_{7/2}$ (980 nm) transition for $A_3[YbL^5_3]$ (Figure 9a). In the case of $A_3[NdL^5_3]$, the $^4F_{3/2} \rightarrow {}^4I_{11/2}$ (1064 nm) and the $^4F_{3/2} \rightarrow {}^4I_{13/2}$ (1327 nm) transitions can be seen (Figure 9b), while the $^4F_{3/2} \rightarrow {}^4I_{9/2}$ (850 nm) transition is not observed because of the low sensitivity of our detector between 850 and 900 nm. In both cases, a residual CT emission is observed around 600 nm; the quantum yield efficiency of this transition, ϕ_{CT}, is significantly reduced compared to that of the Lu analogues, suggesting that the energy transfer is quite good. These results clearly indicate that the CT strategy can be successfully generalized to NIR emitters.

The luminescence lifetimes of $A_3[YbL^5_3]$ and $A_3[NdL^5_3]$ are 37 and 1.2 μs, respectively. These values are in the same range as those of other complexes featuring sensitization via a singlet state; in those cases, the antenna chromophores (dansyl and lyssamine) are not directly linked to the metal, and a through space mechanism is invoked.[64,65] However, these lifetimes are very short compared to the longest obtained for molecular complexes, such as those comprising perfluorinated imidophosphinate ligands ($\tau_{Yb} = 1.11$ ms and $\tau_{Nd} = 44$ μs).[66] These results indicate that the ligand L^5 is not fully optimized either for the sensitization of NIR emitters or for preventing nonradiative decay (via C−H oscillator, for example). Keeping in mind that the complete optimization performed in the case of europium shows that the relaxed CT excited state must be close to the lanthanide accepting

(64) Vögtle, F.; Gorka, M.; Vicinelli, V.; Ceroni, P.; Maestri, M.; Balzani, V. *ChemPhysChem* **2001**, *2*, 769–773.
(65) Hebbink, G. A.; Klink, S. I.; Grave, L.; OudeAlink, P. G. B.; van Veggel, F. C. J. M. *ChemPhysChem* **2002**, *3*, 1014–1018.
(66) Glover, P. B.; Bassett, A. P.; Nockemann, P.; Kariuki, B.; van Deun, R.; Pikramenou, Z. *Chem.—Eur. J.* **2007**, *13*, 6308–6320.

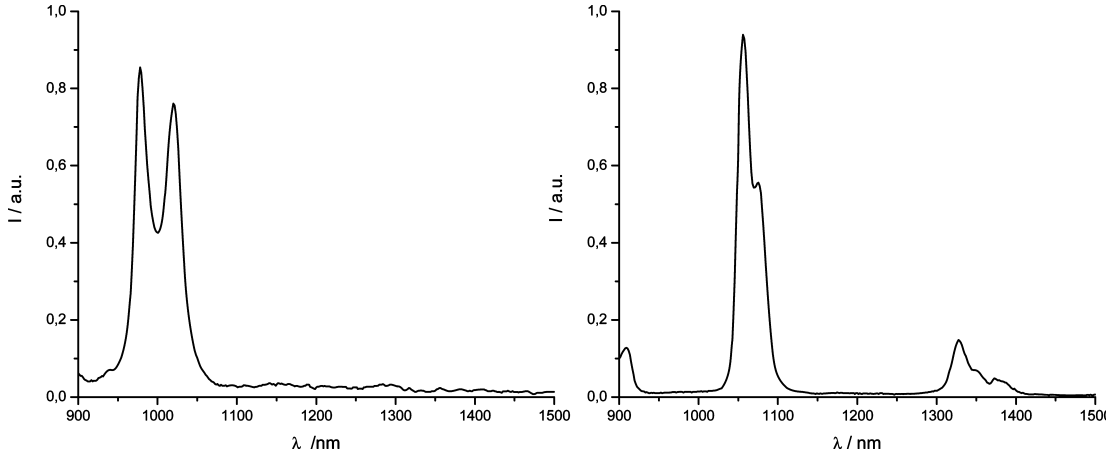

Figure 9. Room temperature emission spectra of $A_3[Yb\mathbf{L}^5{}_3]$ (left) and $A_3[Nd\mathbf{L}^5{}_3]$ (right) in dichloromethane solution ($\lambda_{ex} = 360$ nm).

level, ligands featuring more red-shifted CT transitions should be more appropriate for Nd or Yb sensitization. Further ligand engineering is currently being performed in our group to determine this optimum CT energy level for the sensitization of NIR emitters.

Conclusion

In conclusion, this article unambiguously demonstrates that ligands featuring a charge transfer state can behave as antennae for the direct sensitization of Eu(III), Yb(III), and Nd(III) luminescence in the visible and near-infrared spectral ranges. In the case of europium, very high quantum yields, about 40%, have been reached, underlining the efficiency of this sensitization process. In addition, keeping in mind that CT transitions present generally very strong extinction coefficients, such quantum yields will lead to exceptional brightness (defined as the $\phi \times \varepsilon$ product), which is of prime importance for further application as bioprobes, for instance. In the particular case of functionalized tris-dipicolinate europium complexes, the energy level of the CT donating state has been tuned using solvents or temperature effects and by changing the nature of the electron-donating group. This complete study has allowed to approximate both the lower limit and the optimal energy suitable for Eu(III) sensitization, close to the $^5D_0$ and $^5D_1$ metal accepting states, respectively. More generally, this CT sensitization process opens the way for the design of Ln complexes featuring high nonlinear optical properties, in particular, high two-photon cross-sections (see part 2 paper) and will trigger future development of new bioprobes combining the intrinsic advantages of lanthanide luminescence with those of two-photon excited luminescence microscopy.

Experimental Section

Luminescence. The luminescence spectra were measured using a Horiba-Jobin Yvon Fluorolog-3 spectrofluorimeter, equipped with a three-slit double-grating excitation and emission monochromator with dispersions of 2.1 nm/mm (1200 grooves/mm). The steady-state luminescence was excited by unpolarized light from a 450W xenon CW lamp and detected at an angle of 90° for diluted solution measurements (10 mm quartz cuvette) by a red-sensitive Hamamatsu R928 photomultiplier tube. Spectra were reference-corrected for both the excitation source light intensity variation (lamp and grating) and the emission spectral response (detector and grating). Uncorrected near-infrared spectra were recorded using a liquid-nitrogen-cooled, solid indium/gallium/arsenic detector (850−1600 nm). Phosphorescence lifetimes (>30 μs) were obtained by pulsed excitation using a FL-1040 UP xenon lamp. Luminescence decay curves were fitted by least-squares analysis using Origin. Fluorescence quantum yields, Q, were measured in a diluted water solution with an optical density lower than 0.1 using the following equation $Q_x/Q_r = [A_r(\lambda)/A_x(\lambda)][n_x{}^2/n_r{}^2][D_x/D_r]$, where A is the absorbance at the excitation wavelength (λ), n is the refractive index, and D is the integrated luminescence intensity. The "r" and "x" stand for reference and sample. Here, references are quinine bisulfate in 1 N aqueous sulfuric acid solution ($Q_r = 0.546$) and $[Ru(bpy)_3]Cl_2$ in aqueous solution ($Q_r = 0.028$) for the Lu and Eu complexes, respectively (except for $A_3[Lu(\mathbf{L}^5)_3]$ and $A_3[Lu(\mathbf{L}^6)_3]$, which were measured versus $[Ru(bpy)_3]Cl_{2(aq)}$).[67] The quantum yields were measured three times for the Lu, and for the Eu, they were corroborated by measurements, one respective to the other. Excitation of the reference and sample compounds was performed at the same wavelength.

In the case of the NIR emitters, the sample was excited using a pulsed Nd:YAG laser (SpectraPhysics), operating at 10 Hz. Light emitted at right angles to the excitation beam was focused onto the slits of a monochromator (PTI120), which was used to select the appropriate wavelength. The growth and decay of the luminescence at selected wavelengths was detected using a germanium photodiode (Edinburgh Instruments, EI-P) and recorded using a digital oscilloscope (Tektronix TDS320) before being transferred to a PC for analysis. Luminescence lifetimes were obtained by iterative reconvolution of the detector response (obtained by using a scatterer) with exponential components for growth and decay of the metal-centered luminescence, using a spreadsheet running in Microsoft Excel. The details of this approach have been discussed elsewhere.[68]

Computational Details. DFT geometry optimizations and TD-DFT excitation energy calculations on $\mathbf{L}^i$ ($i = 1-6$) featuring simplified $-OCH_2CH_2OMe$ end groups were carried out with the

(67) Demas, J. N.; Crosby, G. A. *J. Phys. Chem.* **1971**, *75*, 991–1024.
(68) Beeby, A.; Faulkner, S. *Chem. Phys. Lett.* **1997**, *266*, 116–122.

Gaussian 03 (revision B.04) package,[69] employing the three-parameter hybrid functional of Becke based on the correlation functional of Lee, Yang, and Parr (B3LYP).[70,71] The 6-31G* basis sets were used for all atoms.

Acknowledgment. The authors are grateful to the French Agence Nationale de la Recherche (ANR LnOnL NT05-3_42676) for financial support.

Supporting Information Available: Luminescence data in chloroform, details of the equation system resolution, and complete theoretical calculation data. This material is available free of charge via the Internet at http://pubs.acs.org.

IC8012969

(69) Frisch, M. J.; Trucks, G. W.; Schlegel, H. B.; Scuseria, G. E.; Robb, M. A.; Cheeseman, J. R., Jr.; Vreven, J. A. T.; Kudin, K. N.; Burant, J. C.; Millam, J. M.; Iyengar, S. S.; Tomasi, J.; Barone, V.; Mennucci, B.; Cossi, M.; Scalmani, G.; Rega, N.; Petersson, G. A.; Nakatsuji, H.; Hada, M.; Ehara, M.; Toyota, K.; Fukuda, R.; Hasegawa, J.; Ishida, M.; Nakajima, T.; Honda, Y.; Kitao, O.; Nakai, H.; Klene, M.; Li, X.; Knox, J. E.; Hratchian, H. P.; Cross, J. B.; Adamo, C.; Jaramillo, J.; Gomperts, R.; Stratmann, R. E.; Yazyev, O.; Austin, A. J.; Cammi, R.; Pomelli, C.; Ochterski, J. W.; Ayala, P. Y.; Morokuma, K.; Voth, G. A.; Salvador, P.; Dannenberg, J. J.; Zakrzewski, V. G.; Dapprich, S.; Daniels, A. D.; Strain, M. C.; Farkas, O.; Malick, D. K.; Rabuck, A. D.; Raghavachari, K.; Foresman, J. B.; Ortiz, J. V.; Cui, Q.; Baboul, A. G.; Clifford, S.; Cioslowski, J.; Stefanov, B. B.; Liu, G.; Liashenko, A.; Piskorz, P.; Komaromi, I.; Martin, R. L.; Fox, D. J.; Keith, T.; Al-Laham, M. A.; Peng, C. Y.; Nanayakkara, A.; Challacombe, M.; Gill, P. M. W.; Johnson, B.; Chen, W.; Wong, M. W.; Gonzalez, C.; Pople, J. A. *Gaussian 03*, revision B.04; Gaussian, Inc.: Pittsburgh, PA, 2003.

(70) Lee, C. T.; Yang, W. T.; Parr, R. G. *Phys. Rev. B: Condens. Matter Mater. Phys.* **1988**, *37*, 785–789.

(71) Becke, A. D. *J. Chem. Phys.* **1993**, *98*, 5648–5652.